

Mobile capacity enhancement using unequally spaced antenna arrays

Rittwik Jana
Department of Systems Engineering
The Australian National University
Canberra, ACT 0200, Australia.
email: rittwik@syseng.anu.edu.au

Subhrakanti Dey, *Member, IEEE*
Department of Systems Engineering
The Australian National University
Canberra, ACT 0200, Australia.
email: subhra@syseng.anu.edu.au

Abstract - Adaptive arrays can significantly increase cell capacity, improve signal quality, and reduce transmitter power requirements. In this paper, we investigate the capacity improvement that can potentially be achieved via an optimised design strategy for an *unequally spaced* array. We also investigate the effect that fading correlation has on the performance of an unequally spaced adaptive array. Results are presented for optimum combining with flat fading. Computer simulations show that it is possible to achieve a gain of at least 1.5 dB for moderate to high signal-to-noise ratios (SNR) when compared to the equally spaced array.

I. Introduction

Future wireless communication systems have to support not only speech but also Internet and multimedia communication. This implies a tremendous increase in system capacity demand. One way of achieving the increase in capacity is to introduce smart antenna systems. These are systems in which the base station antennas do not have a fixed pattern, but adapt to the current radio conditions. There are three different smart antenna concepts, namely, switched lobe array, phased array and adaptive antenna arrays. In this paper we use adaptive antenna arrays with unequal element spacings and evaluate the potential capacity improvements one can achieve under various channel conditions. We establish a relationship between the information theoretic capacity and the beam pattern of a multi-sensor array. Specifically, we investigate the potential capacity enhancement obtainable via an optimised design for an *unequally spaced* antenna array. We optimise the positions and the weighting coefficients of the array elements to simultaneously improve the capacity subject to a constraint on the height of the maximum sidelobe and/or minimise the width (beamwidth) of the main lobe. We illustrate with examples realisable gains when compared to the equally spaced conventional design. We also investigate the performance of an unequally spaced array in a multipath fading environment. Optimum combining and signal processing with multiple antennas is not a new idea [4],[5]. In

this paper, we use similar techniques to quantify the reduction in the average bit error rate (BER) for a system with $N = 3$ users and 4 antenna elements in a flat Rayleigh fading environment. It is seen that an effective improvement of 1.5dB is obtained for moderate to high SNRs. For a large number of elements, a probabilistic methodology, namely simulated annealing [2], is used to solve this complex combinatorial optimisation problem.

II. Beam Pattern Formulation

For a linear array with M uniform and omnidirectional elements placed along the x -axis (see Fig. 1), the beam amplitude $p(u)$ can be expressed as $p(u) = \left| \sum_{i=0}^{M-1} w_i e^{j \frac{2\pi}{\lambda} x_i u} \right|$ where x_i is the position of the i -th element, w_i is the related weight coefficient, $u = \sin\theta - \sin\theta_0$ (θ and θ_0 being respectively the angle of incidence of the plane wave and the steering angle (see Fig. 1)), and $\lambda = 2\pi c/w$, $u \in [-2, 2]$. All signals arrive at the base station within $\pm\Delta$ of θ_0 . The normalised beam power (also known as the beam pattern), $P(u)$ can also be written as

$$P(u) = \left(\frac{p(u)}{Q} \right)^2 \quad (1)$$

where Q is the sum of all w_i 's. Each sensor has a complex weight and a carrier phase associated with it. The position of the main beam can be steered by varying the amplitudes and phases of these sensor weights. The simplest choice of sensor weights is uniform (i.e., identical amplitudes and phases). Throughout this paper, the spatial aperture, 6λ is fixed. Thus for an equally spaced array with 4 elements, the positions of the elements are at $[0 \ 2\lambda \ 4\lambda \ 6\lambda]$.

III. Multiuser Information Capacity

The channel capacity, C (in bits/sec), for an AWGN channel with bandwidth, B , signal power, P , and noise power, σ^2 , is given by the Shannon formula,

$$C = B \log_2 \left(1 + \frac{P}{\sigma^2} \right) \quad (2)$$

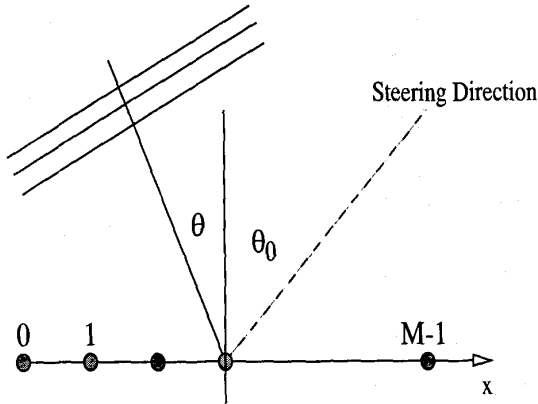


Figure 1: Geometry and notations used for a linear array

In the case of one interfering user with a received signal power identical to that of the desired user, the capacity can be written as

$$C(u) = B \log_2 \left(1 + \frac{P(u_{max})}{P(u) + \sigma^2} \right) \quad (3)$$

where $P(u_{max})$ is the maximum power in the direction of the main beam u_{max} coincident with the direction of the desired user's signal and $P(u)$ denoting the power of the interfering user's signal arriving from a direction, u . The maximum capacity, C_{max} , for a system with one interfering user occurs when the interfering user's signal is suppressed totally by nulls (i.e., $P(u) = 0$) in the beam pattern.

$$C_{max} = B \log_2 \left(1 + \frac{P(u_{max})}{\sigma^2} \right) \quad (4)$$

Similarly, the minimum capacity, C_{min} is obtained when the interfering signal power is also $P(u_{max})$ (i.e., the interferer is present inside the main beam). This is analogous to the situation when there is only one sensor (i.e., no array).

$$C_{min} = B \log_2 \left(1 + \frac{P(u_{max})}{P(u_{max}) + \sigma^2} \right) \quad (5)$$

A more detailed discussion on the implications of these results can be found in [3]. In this paper, we maximise the expected system capacity, $E\{C(u)\}$, given by

$$E\{C(u)\} = \int_{-2}^2 C(u) f_u(u) du \quad (6)$$

where $f_u(u)$ is the probability density function of u , where $u = \sin \theta - \sin \theta_0$. For an AMPS system, the

p.d.f. of θ has been shown to be [1]

$$f_\theta(\theta) = \begin{cases} \frac{2D \cos(\theta) \sqrt{D^2 \cos^2(\theta) - D^2 + R^2}}{\pi R^2}, & -\arcsin\left(\frac{R}{D}\right) \leq \theta \leq \arcsin\left(\frac{R}{D}\right) \\ 0 & \text{otherwise} \end{cases} \quad (7)$$

where D is the distance between the base stations and R is the radius of the cell. A more common approach is to assume the p.d.f. of AOA to be uniform. We shall compare our results for both scenarios.

IV. Performance Analysis

In this section we develop a mathematical model for a multipath environment applicable in wireless digital communications. This model is useful for the evaluation of signal correlations among the antenna array elements. Fig. 2 shows a wireless system with N users, each with an antenna, communicating with a base station with M antennas. The channel trans-

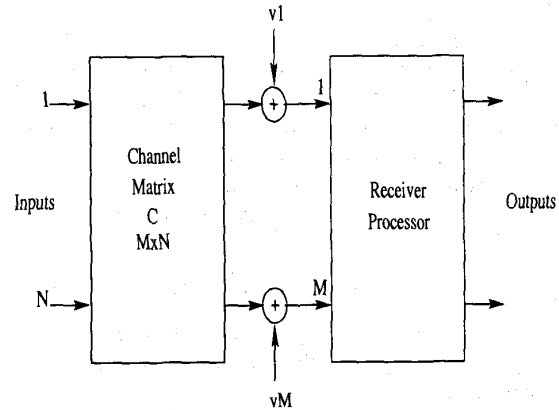


Figure 2: Multiuser communication block diagram

mission characteristics matrix can be expressed as

$$C(\omega) = (C_1(\omega), C_2(\omega), \dots, C_N(\omega)) \quad (8)$$

where ω is the frequency in radians per second, the column vector $C_k(\omega)$ represents the transmission characteristics from user k to all the antenna elements, $C_k(\omega) = [c_{k1}(\omega), \dots, c_{kM}(\omega)]^T$. Since each user is characterised by its own surroundings, and if the users are not on top of one another to within wavelengths, it is reasonable to assume that the columns in (8) are statistically independent. The correlation of fading between two antenna spaced d apart is given by [7]

$$R_{xx} = \int_{-\frac{\pi}{2} + \phi}^{\frac{\pi}{2} + \phi} \cos(2\pi d / \lambda \sin(\phi_i - \phi)) p(\phi_i) d\phi_i \quad (9)$$

and

$$R_{xy} = \int_{-\frac{\pi}{2} + \phi}^{\frac{\pi}{2} + \phi} \sin(2\pi d / \lambda \sin(\phi_i - \phi)) p(\phi_i) d\phi_i \quad (10)$$

where $\lambda = \omega/(2\pi c)$, c is the speed of light, R_{xx} is the correlation between the real parts of c_{ij} and c_{ik} , R_{xy} is the correlation between the real part of c_{ij} and the imaginary part of c_{ik} and ϕ_i is the steering angle. At the receiver, the M receive signals are linearly combined to generate the output signals. We are interested in the performance of this system with the optimum linear combiner, that combines the received signal to minimise the mean squared error (MSE) for user 1 in the output. An explicit expression for the MSE is

$$MSE[C] = \sigma_a^2 \frac{T}{2\pi} \int_{-\pi/T}^{\pi/T} \left[I + \frac{C^\dagger(\omega)C(\omega)}{N_0} \sigma_a^2 \right]_{11}^{-1} d\omega \quad (11)$$

where $\sigma_a^2 = E|a_n^{(1)}|^2$, $[\cdot]_{11}^{-1}$ stands for the 1 1 component of the matrix, T is the symbol duration, N_0 is the noise density, a_n 's are the 1st user's complex data symbols.

Flat Rayleigh Fading

In this section we present well known results [6] to compute the probability of error for flat fading environments. With multipath, the $c_{ij}(\omega)$'s are modelled as complex Gaussian random variables at each frequency ω . The variation of $c_{ij}(\omega)$ depends on the delay spread model of the channel. For flat fading, $c_{ij}(\omega) = c_{ij}$ for all ω . Under this condition the "zero forcing" optimum combiner solution reduces to

$$MSE[C] = (C^\dagger C)^{-1}_{11} N_0 \quad (12)$$

Using the MSE given by (12) an exponentially tight upper bound on the conditional probability of error is given by [6]

$$P_e(C) \leq \exp \left\{ -\frac{\rho}{\sigma_a^2} \frac{1}{(C^\dagger C)^{-1}_{11}} \right\} \quad (13)$$

where ρ is the SNR for user "1" i.e. $\rho = \frac{\sigma_a^2 \sigma_1^2}{N_0}$. To compute the probability of error we only need to characterise the correlation properties of a typical user. By expressing the complex column vector $C_k(\omega) = \mathbf{x}_k(\omega) + i\mathbf{y}_k(\omega)$, where \mathbf{x}_k and \mathbf{y}_k are the real and imaginary M -column vectors associated with user k . Define a $2M$ augmented column vector as

$$\Gamma_k = (\mathbf{x}_{k1} \ \mathbf{y}_{k1} \ \dots \ \mathbf{x}_{kM} \ \mathbf{y}_{kM})' \quad (14)$$

and evaluate the $2M \times 2M$ correlation matrix

$$R_k = E \left[\Gamma_k^\dagger \Gamma_k \right], \quad k = 1, \dots, N \quad (15)$$

It can be easily seen that R_k can be represented in the form

$$\frac{R_k}{\sigma_k^2} = \begin{bmatrix} I_{2 \times 2} & D_1 & D_2 & \dots & D_M \\ D_1^T & I_{2 \times 2} & D_1 & \dots & D_{M-1} \\ D_2^T & D_1^T & I_{2 \times 2} & \dots & D_{M-2} \\ \vdots & \vdots & \vdots & \ddots & \vdots \\ D_M^T & D_{M-1}^T & D_{M-2}^T & \dots & I_{2 \times 2} \end{bmatrix} \quad (16)$$

where σ_k^2 is the received signal power for the k th user and

$$D_{|i-j|} = \begin{bmatrix} R_{xx}(i-j) & R_{xy}(|i-j|) \\ -R_{xy}(|i-j|) & R_{yy}(i-j) \end{bmatrix} \quad (17)$$

For given ϕ for each user, beamwidth Δ and d/λ , the correlation matrix R_k was evaluated using (15). C was then generated to satisfy R_k .

V. Results and Discussion

In this section we illustrate by simulations the potential improvements in capacity achievable for an optimised unequally spaced antenna when compared to its equally spaced counterpart. The equally spaced array has 4 elements and are spaced at 2λ apart. The positions of the 4 elements were at $X = [x_1 \ x_2 \ x_3 \ x_4]$ with $x_1 = 0, x_4 = 6\lambda$. The remaining elements x_2 and x_3 , could assume any position within an interval of 0.1λ . The signal-to-noise power ratio ($SNR = \frac{P(u_m a x)}{\sigma_a^2}$) was set to 100. The weighting functions were all identical.

Fig. 3 plots the expected capacity for varying position increments of x_2 and x_3 . It is seen that the maximum capacity is obtained when $x_2 = 0.6$ and $x_3 = 5.4$, (i.e., $X = [0 \ 0.6 \ 5.4 \ 6]$). The capacity for the unequally spaced array is 4.22 an increase of 32% over the equally spaced array (capacity = 3.2). Fig.

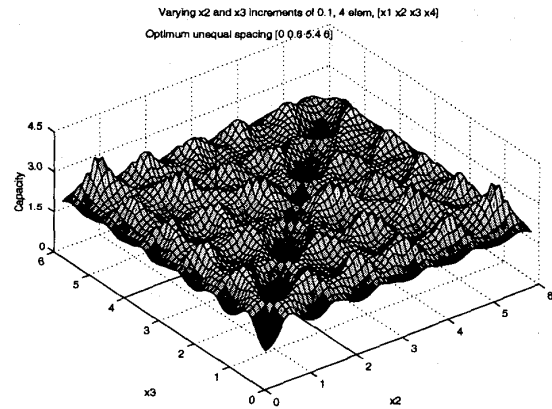


Figure 3: Plot of the capacity surface versus varying antenna positions, uniform p.d.f. of $f_u(u)$

4 plots the capacity surface for the previous example however, for a non-uniform p.d.f.. Specifically we use a reuse factor of 1 in (7). Clearly the p.d.f. of the AOA of the interfering users shapes the capacity surface differently. The maximum capacity is obtained for $X = [0 \ 1.2 \ 4.8 \ 6]$ ($C_{max} = 3.76$).

It is important to note that the average system capacity is not the only criterion that determines the

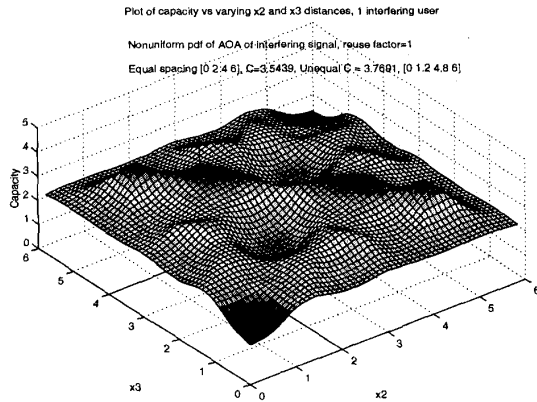


Figure 4: Plot of the capacity surface versus varying antenna positions, non-uniform p.d.f. of $f_u(u)$, $N=1$

efficiency of the system. The height of the maximum sidelobe and the width of the main beam also determines the effective interference rejection capability. Fig. 5 plots the maximum sidelobe levels versus different antenna positions. An equally spaced array has a maximum sidelobe level of $0dB$ due to the presence of the grating lobes at ± 90 degrees. For an unequally spaced array the maximum sidelobe level is $-4.13dB$ at $X = [0 \ 0.8 \ 2.5 \ 6]$. However, the capacity for this configuration is only 2.98. It is difficult to realise a maximum capacity and a minimum sidelobe level for the same antenna geometry. By

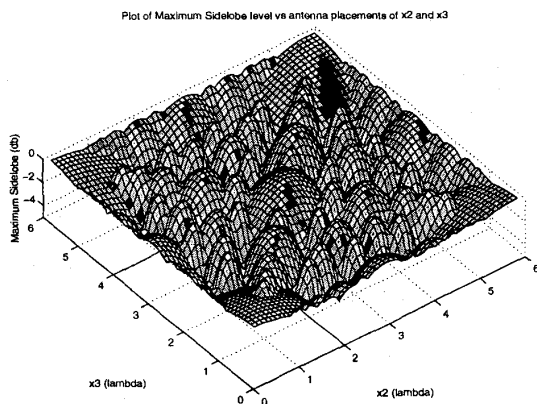


Figure 5: Plot of the maximum sidelobe level versus varying antenna positions, uniform pdf

adjusting the weights it is now possible to further reduce the maximum sidelobe. It is well known that the Weiner-Hopf solution is identical to the maximum SNR solution for a narrow band emission from a single source in the absence of multipath effects

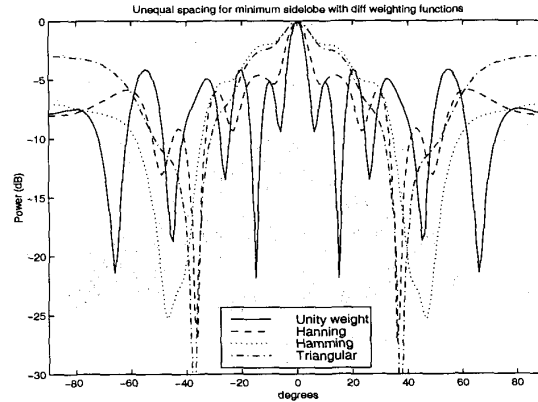


Figure 6: Maximum sidelobe reduction for various windowing functions

and other complications. The signal from a source may arrive via several paths of different time delays and attenuations. The LMS algorithm, by definition, finds the best weighting vector in the output SNR sense for an arbitrary input signal and multipath is not expected to be a serious problem here unless the various desired signal arrivals are fluctuating so rapidly that the algorithm cannot follow the changes fast enough. This is particularly likely to be the case if the desired signal is very weak for its convergence. The problems associated with multipath of the interference signals is worth noticing, the main effect being that the antenna must steer nulls at several sources rather than one for each interference transmitter. Fig. 6 shows further suppression of the maximum sidelobe to $-5dB$ using a Hanning window, however, at the expense of an increased beamwidth.

The beamwidth plot delineates distinct regions of beamwidth levels. It is intuitive that as the elements are placed closer to the end of the array, the beamwidth decreases. However, for large portions of the optimisation surface, the beamwidth remains relatively constant.

Performance with Fading and Interference

It is important to investigate the performance of an unequally spaced adaptive array under the effect of channel fading. Fig. 8 considers the effect of correlation with flat fading for equally spaced arrays. It is seen that the BER improves as the spacing between the elements increases. This suggests that it may be possible to improve the error rate with unequally spaced arrays which aims to increase the average d/λ . Increasing the antenna spacing by a factor of 10 decreases the tolerable Δ by a factor of 10 as well. However for very small beamwidth, the

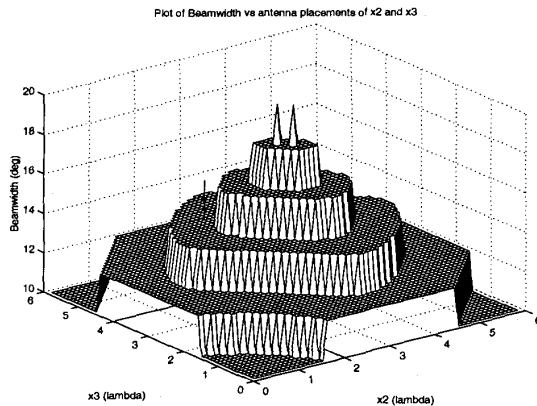


Figure 7: Plot of the beamwidth level versus varying antenna positions, uniform pdf

BER worsens rapidly. Fig. 8 also shows the degradation in performance as the interference increases (i.e., $M = N = 3$, $X = [0 \ 0.382 \ 0.764]$). Fig. 9

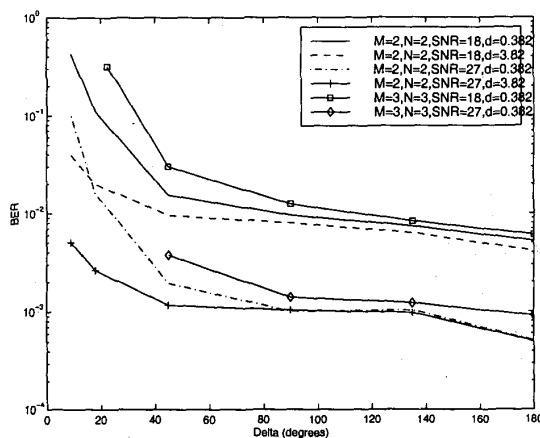


Figure 8: Average error rate versus Δ with flat fading

shows the effective gain in SNR for an optimised unequal spaced array with 4 elements when compared to the equally spaced array under flat fading conditions. At a BER of 5×10^{-3} the unequal spaced design outperforms the equally spaced array by 1.5 to 2 dB.

Thanks to the high flexibility of simulated annealing (SA) [2], one can do this complex combinatorial optimisation for a large number of array elements. SA allows one to optimise the positions and the weight coefficients at the same time and in parallel. The optimised configuration was for $X = [0.0 \ 17.0 \ 17.4 \ 17.7 \ 22.3 \ 15.9 \ 44.4 \ 32.4 \ 15.3 \ 16.6 \ 19.2 \ 12.7 \ 27.5 \ 45.0 \ 21.5 \ 7.9 \ 26.7 \ 27.1 \ 29.1 \ 13.5 \ 19.5 \ 14.6 \ 37.1$

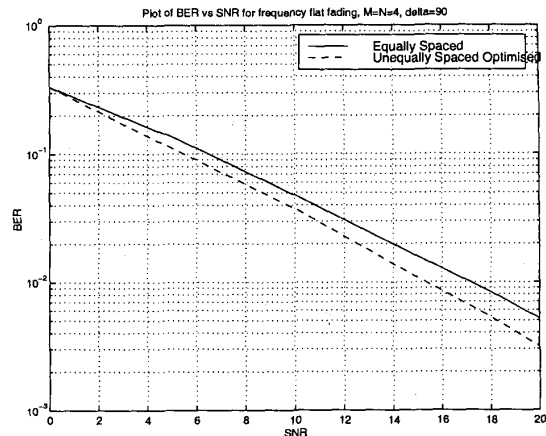


Figure 9: Plot of BER vs SNR for unequal spaced and equally spaced array

14.9 50.0]. The capacity was 1.70 bits/sec/Hz. In comparison the equally spaced array was only 1.42 bits/sec/Hz.

References

- [1] P. Petrus, R. B. Ertel and J. H. Reed, "Capacity enhancement using adaptive arrays in an AMPS system," *IEEE Trans. on Vehicular Technology*, vol. 47:3, pp.717-727, Aug. 1998.
- [2] V. Murino, A. Trucco and C. S. Regazzoni, "Synthesis of an equally spaced arrays by simulated annealing," *IEEE Trans. on Signal Processing*, vol. 44, pp. 119-123, Jan. 1996.
- [3] P. B. Rapajic, "Information capacity of the space division multiple access mobile communication system," *Wireless Personal Communications*, pp.131-159, 199.
- [4] J. H. Winters, "Optimum combining for indoor radio systems with multiple users," *IEEE Trans. on Communications*, pp.1222-1230, Nov. 1987.
- [5] J. H. Winters, "On the capacity of radio communications systems with diversity in a Rayleigh fading environment," *IEEE Journal of Selected Areas in communications*, pp.871-878, June 1987.
- [6] J. H. Winters, J. Salz, R. D. Gitlin, "The impact of antenna diversity on the capacity of wireless communication systems," *IEEE Trans. on Communications*, pp.1740-1750, Feb/Mar/Apr 1994.
- [7] W.C.Y. Lee, "Effects on correlation between two mobile radio base station antennas," *IEEE Trans. on Communications*, vol. COM-21, pp.1214-1224, Nov. 1973.